FACTA UNIVERSITATIS
Series: **Electronics and Energetics** Vol. 37, Nº 4, December 2024, pp. 639 – 654
https://doi.org/10.2298/FUEE2404639M

Original scientific paper

ON THE DESIGN OF PASSIVE DISPERSIVE FILTERS FOR ANALOG SIGNAL PROCESSING APPLICATIONS*

Hanane Meliani[1], Emilie Avignon-Meseldzija[1], Jelena Anastasov[2], Dejan N. Milic[2], Pietro Maris Ferreira[1]

[1]Université Paris-Saclay, CentraleSupélec, Sorbonne-Université, CNRS, Lab. de Génie Electrique et Electronique de Paris
[2]Faculty of Electronic Engineering, University of Niš, Aleksandra Medevedeva 4, 18104 Niš, Serbia

ORCID iDs:	Hanane Meliani	https://orcid.org/0009-0006-2118-3880
	Emilie Avignon-Meseldzija	https://orcid.org/0000-0001-5268-9223
	Jelena Anastasov	https://orcid.org/0000-0002-8200-4130
	Dejan Milic	https://orcid.org/0000-0001-6472-2027
	Pietro Maris Ferreira	https://orcid.org/0000-0002-0038-9058

Abstract. *The paper presents the design of two dispersive filters (also called phasers) dedicated to Analog Signal Processing (ASP) applications. Possible ASP applications targeted for these filters are also proposed: analog pulse compression radar, analog chirp Fourier transformer and frequency discriminator. In the past decades, dispersive filters for ASP have been implemented with Surface Acoustic Wave (SAW) filters, having a reduced bandwidth leading to a poor resolution in the applications. Consequently, designing these filters with a larger bandwidth is a significant progress and this is what is proposed in this work. The design of the two filters is described step-by-step: the mathematical method employed to optimize the parameters of the filters, the calculation of theoretical values of components and the selected real values of components of the shelves for the PCB. The two measured filters, composed of 2 passive cells, have negative slope and positive slope group delay characteristics: the first filter has a group delay downslope of -1 ns/GHz for the considered bandwidth [700MHz – 1.9GHz], and the second has a group delay upslope of 1.25ns/GHz for the considered bandwidth [500MHz-1.3GHz].*

Key words: *dispersive filter, phasers, analog signal processing, group delay, analog chirp Fourier transformer, Frequency discriminator*

Received February 16, 2024; revised September 30, 2024; accepted October 09, 2024
Corresponding author: Hanane Meliani
Université Paris-Saclay, CentraleSupélec, Sorbonne-Université, CNRS, Lab. de Génie Electrique et Electronique de Paris (E-mail: Hanane.Meliani@centralesupelec.fr)
*An earlier version of this paper was presented at the 16th International Conference on Advanced Technologies, Systems and Services in Telecommunications (TELSIKS 2023), October 25-27, 2023, Niš, Serbia [1]

1. INTRODUCTION

Most of the receivers in communication and radars nowadays are built on the idea that the signal processing will be achieved in the digital domain. The analog front end is, most of the time, reserved to the signal conditioning (mostly amplification, filtering and multiplication) before the analog-to-digital conversion (ADC). In this approach one of the most power-hungry blocks is the ADC, especially when considering very large bandwidth signal to be digitized. This is why a new research trend consists in rethinking the receiver architectures with direct Analog Signal Processing (ASP). The authors in [2] conducted an extensive overview of the different techniques to achieve signal processing dedicated to telecommunication systems directly in the analog domain. Among the numerous approaches to achieve ASP, including Analog Spiking Neural Networks [3] and Analog-FTT [4], we focus in this article on phasers-based ASP systems [5]. The signal processing operations that can be achieved directly in the analog domain with phasers-based systems are for example: analog pulse compression, analog chirp Fourier transform and frequency discrimination for real time spectrum analysis. As its name indicates, the key component for any of these signal processing applications is the phaser, which is a dispersive filter. A dispersive filter attributes a specific delay for a specific frequency. Several techniques have been considered to obtain such filters, each of these techniques having strengths and limitations. In the eighties these kinds of filters have been implemented with Surface Acoustic Wave (SAW) filters [6]. Unfortunately, despite the large dispersion that can be obtained, they present a reduced bandwidth and are then not suitable for nowadays communication and radar applications. In optical communication, where there is a need for sharp optical pulses, the tendency is to time compression with optical phasers [7, 8]. These optical devices are very bulky and would not be compatible with traditional telecommunication systems or embedded applications. In electronics and microwave techniques, many attempts to implement these arbitrary group delay engineered filters with passive LC topologies, active CMOS integrated technologies or microstrip lines have been published with variable performances [9-14]. One of the most challenging part of the design of such filters is the optimization of parameters to obtain a linear group delay versus frequency. Several methods have been proposed [9, 15, 16] very sensitive to group delay initialization.

In what comes next, we propose to design downslope and upslope linear group delay dispersive filters for possible use in applications in Analog Signal Processing with the robust optimization method proposed in [17] and we use components of the shelves soldered on PCBs.

The paper is organized as follows: Section II presents possible phasers-based ASP applications for the dispersive filter. Section III presents two optimized upslope and downslope dispersive filters suitable for these kinds of applications and Section IV presents measurement results of the realized filters.

2. PHASERS-BASED ANALOG SIGNAL PROCESSING APPLICATIONS

2.1. State-of-the-art of phasers-based analog signal processing applications

Many attempts have been conducted the last decades to implement various phasers-based ASP. Most of these attempts concerns real-time spectrum analysis. For these real-time spectrum analysis, we can distinguish several architectures. The first architecture is the spectrum sniffer [18-20]. The spectrum sniffer is based on a phaser having a stepped

group delay response versus frequency. It means that a given frequency bandwidth has several channel bandwidths having each a different group delay. Consequently, when a signal goes through this spectrum sniffer, we obtain at the output a signal decomposed in time, depending on which frequency bandwidths were present at the input. The principle is the same for the frequency discriminator excepts that for this latter the group delay is linear versus frequency [21]. Another architecture for rel-time spectrum analysis is the Analog Chirp Fourier Transformer described later in what follows in section 2.3. Several attempts of implementing this architecture have been published in [22-25].

An interesting attempt of implementing phasers-based systems concerns UWB communication techniques [26]. In this work, communication pulses are transformed through a dispersive filter into UWB (Ultra Wide Band) signals whose properties depends on the dispersive filters properties. Thus, only an appropriate dispersive filter, mathematically calculated, can retrieve the original signal. It is a temporal expansion paving the way to UWB fully-analog communication.

Several attempts of temporal expansion have also been conducted with phasers [27, 28] to slow down an RF signal in order to make it easier to sample it for further processing. Another example of temporal manipulation is the work published in [29], where a time reversal mirror has been implemented with a phaser.

In what follows, we will describe more precisely the following phasers-based systems: the analog pulse compression radar, the analog chirp Fourier transformer and the frequency discriminator.

2.2. Analog Pulse Compression Radar

For embedded short-range detection, FMCW (Frequency Modulated Continuous Wave) radars are generally preferred to their pulse-radar counterpart due to the relative simplicity to emit a chirp signal compared to a short-time high-power pulse. In a large majority of FMCW radar architectures, the sent chirp is multiplied with the received chirp to obtain a beat signal whose frequency is proportional to the distance [30, 31]. The beat signal is then digitized and processed in the frequency domain, most of the time by FFT. A possible alternative to the architecture with the multiplier, implemented in the eighties with SAW filter, is the one with an analog matched filter [32] as presented in Figure 1. The emitter of the analog pulse compression radar is composed of a chirp generator creating the signal $s(t)$ and a PA (Power Amplifier). The receiver is composed of a LNA (Low Noise Amplifier) and an analog matched filter. Ideally, the analog matched filter is a filter whose impulse response $h(t)$ is a complex-conjugated and time-reversed version of $s(t)$. The group delay $\tau(f)$ of the matched filter must attribute a specific delay to each frequency in order to achieve the compression. For example, if we have a linear up-chirp signal $s(t)$, then the group delay $\tau(f)$ of the matched filter must be with linear negative slope. At the output of the matched filter we obtain a pulse corresponding to the time reference due to the chirp applied without delay and pulses corresponding to delayed chirps from target feedbacks. To exploit this output, it is possible to place a comparator and a counter to evaluate the delay $2d/c$ proportional to the distance d.

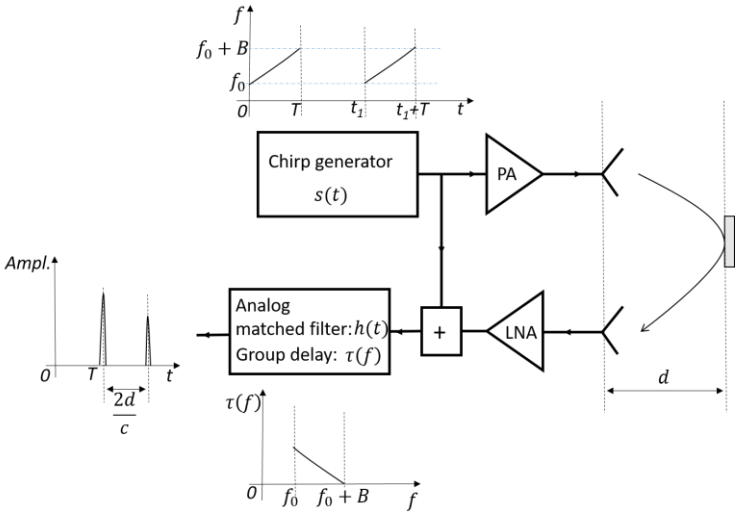

Fig. 1 Analog Pulse Compression Radar

For the sake of simplicity, we will consider all the signals as ideal complex signals (manipulating exponential signal is easier and is the ideal reference). The transmitted up-chirp signal is

$$s(t) = Ae^{i2\pi\left(f_0 t+\frac{1}{2}at^2\right)} \tag{1}$$

where f_0 is the initial frequency of the chirp and a is the ratio B/T with B the bandwidth of the chirp and T the sweep time of the chirp. Let's consider that the chirp is reflected by a target at a distance d, corresponding to a delay in the received chirp $\tau_0 = 2d/c$. Then, we have at the input of the matched filter

$$e(t) = Ae^{i2\pi\left(f_0 t+\frac{1}{2}at^2\right)} + A_0 e^{i2\pi\left(f_0(t-\tau_0)+\frac{1}{2}(t-\tau_0)^2\right)} \tag{2}$$

The impulse response of the matched filter is

$$h(t) = e^{i2\pi\left(f_2 t-\frac{1}{2}at^2\right)} \tag{3}$$

where $f_2 = f_0 + B$. The output of the filter $Out(t)$ is then the convolution of $h(t)$ with $e(t)$

$$Out(t) = \int_0^{2T} h(x)e(t-x)dx \tag{4}$$

Leading to

$$Out(t) = Ae^{i2\pi\left(f_0 t+\frac{1}{2}at^2\right)}\operatorname{sinc}(2B(T-t)) + A_0 e^{i2\pi\left(f_0(t-\tau_0)+\frac{1}{2}a(t-\tau_0)^2\right)}\operatorname{sinc}(2B(T-t+\tau_0)) \tag{5}$$

From (5), it can be observed that the output signal of the matched filter is composed of two *sinc* functions. One *sinc* function is centered around T and is the time reference for the radar, and the other *sinc* is centered around $T + \tau 0$. So the time difference between the maximum of the two *sinc* is the delay to the target. The distance to the target is then deduced by: $d = \tau_0 c/2$. Due to the distance to the target, the amplitude of the signal reflected by the target is attenuated, this is why the second pulse is always smaller than the reference.

Figure 2 presents the output of the analog matched for two different chirp bandwidths *B*: 1.5 GHz and 5 GHz. The other parameters are: T = 10ns, f_0 = 100 MHz, A = 1, A_0 = 0.7 and a distance to the target d = 30 cm corresponding to a τ_0 of 2 ns. As it is predictable from (5) based on *sinc* function, the principal lobe width decreases with increased chirp bandwidth *B*. It means that the larger is the bandwidth of chirp and matched filter, the better the resolution (i.e as in FMCW radar). One of the limitations in analog pulse compression radar is the achievable bandwidth of the matched filter.

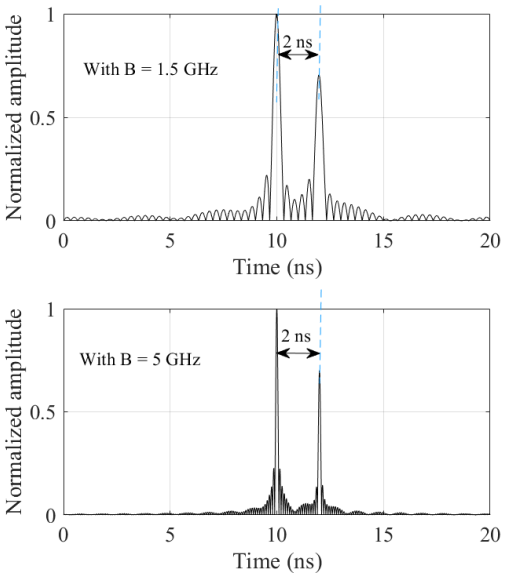

Fig. 2 Output of analog matched filter with B = 1.5 GHz (up) and B = 5 GHz (down)

2.3. Analog Chirp Fourier Transformer

The concept of analog chirp Fourier transformer, based on SAW dispersive filters, has been first published in mid-seventies, beginning of eighties [6, 22, 23]. Due to the limited bandwidth of SAW filters, the concept has been first abandoned and now start to be re-explored with new techniques to design the dispersive filters [24, 25]. The architecture of the analog chirp Fourier transformer is presented in Figure 3. The basic operation of the chirp-transformation consists in the multiplication of the input signal by a complex linearly frequency-modulated waveform $s_a(t)$ (the chirp) followed by the convolution of this product through a filter whose impulse response $h_a(t)$ is a complex chirp of opposite modulation $s_a^*(t)$ leading to:

$$y(t) = (e_a(t) \cdot s_a(t)) * h_a(t) \tag{6}$$

And
$$y(t) = \int e_a(\tau) s_a(\tau) h_a(t-\tau) d\tau \tag{7}$$

with $s_a(t) = e^{-i\pi kt^2}$ and $h_a(t) = e^{i\pi kt^2}$

The convolution of the product then becomes

$$y(t) = \int e_a(\tau) e^{-i\pi k\tau^2} e^{-i\pi k(t-\tau)^2} d\tau \tag{8}$$

which is after development

$$y(t) = e^{i\pi kt^2} \int e_a(\tau) e^{-i2\pi kt\tau} d\tau \tag{9}$$

After multiplying by $s_a(t)$ we finally obtain at the output an expression approaching the Fourier Transform with a Time/Frequency correspondence

$$Out_a(t) = \int e_a(\tau) e^{-i2\pi kt\tau} d\tau \tag{10}$$

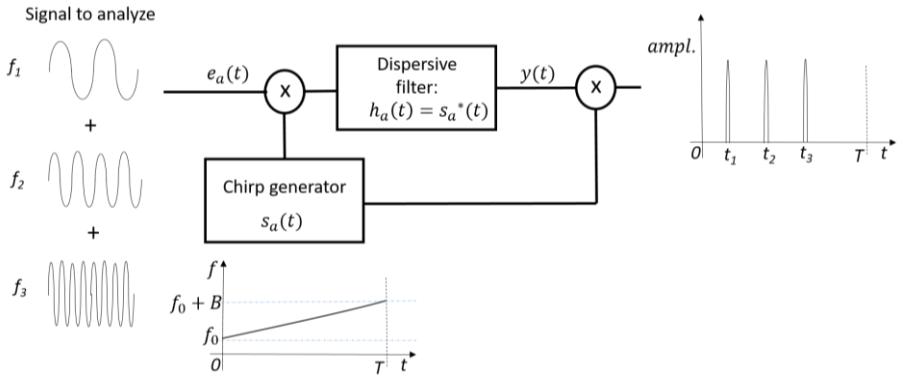

Fig. 3 Architecture of analog chirp Fourier transformer

Figure 4 presents the complex magnitude of the output of an analog chirp Fourier transformer with $k = \Delta f/T = 3 \cdot 10^{16}$, with $\Delta f = 3$ GHz, which is the bandwidth to analyze and $T = 100$ ns the sweep time. At the input we consider the sum of three sinusoidal signals

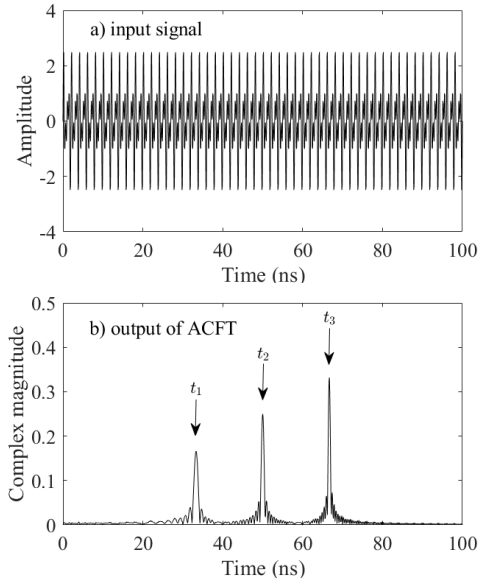

Fig. 4 Input and output of analog chirp Fourier transformer

of frequency f_1 = 1 GHz, f_2 = 1.5 GHz and f_3 = 2 GHz. It can be observed that at the output there are three peaks appearing at t_1 = 33.33 ns, t_2 = 50 ns and t_3 = 66.66 ns corresponding to frequency f_1 =1 GHz, f_2 =1.5 GHz and f_3 = 2 GHz.

2.4. Frequency Discriminator

A frequency discriminator directly exploits the property of the dispersive filter. The dispersive filter attributes a specific delay corresponding to a specific frequency. So if we apply at the input of the dispersive filter a sum of signals at different frequencies f_1, f_2 and f_3 and we multiply it with a Gaussian or triangular pulse, we will obtain at the output several Gaussian or triangular pulse centered around the delays τ_1, τ_2 and τ_3, as illustrated in Figure 5. This principle has been used for example in [19, 20] to create a Real-Time spectrum sensor for cognitive radios. Figure 6 presents the waveform of the input of the filter and the output of the filter to illustrate the method. At the input, we consider the sum of three sinusoidal signals of frequencies f_1 = 1 GHz, f_2 = 1.5 GHz and f_3 = 2 GHz, as for the analog chirp Fourier transformer.

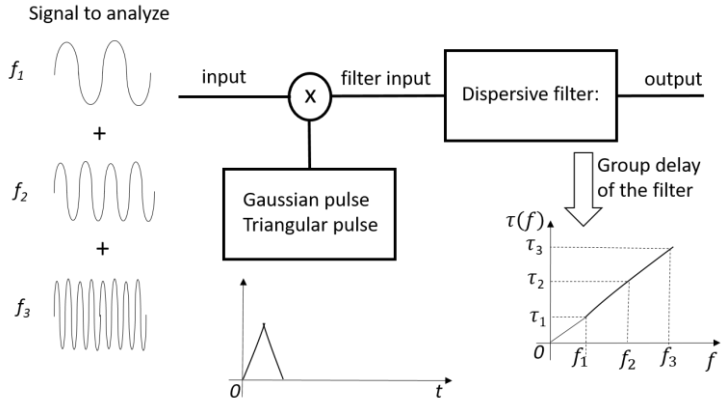

Fig. 5 Architecture of the frequency discriminator

3. Description of the Dispersive Filters

3.1. Optimization of the dispersive filters

The matched filter is a dispersive filter, more particularly with a linear group delay. To calculate the cascade of suitable all-pass cells we will use the most recent and robust mathematical method presented in [17]. This method has been used already to optimize the positive slope active dispersive filters presented in [11]. For a two cells cascade of downslope dispersive filter on the bandwidth 700 MHz – 2 GHz, optimal parameters are proposed in Table 1 and for a two cells cascade of upslope dispersive filter on the bandwidth 500 MHz – 1.3 GHz, optimal parameters are given in Table 2. In these tables the f_{0i} and Q_i refer to the center frequency and quality factor of general second order all pass cell having the transfer function given by (11). The group delay of this filter is the derivative of the phase response with respect to ω, and can be expressed as (12) in

accordance with [33]. This kind of second order filter can be obtained with a passive bridge-T approach like presented in [17] or with an active approach like in [11]. In this work we selected the passive approach and the synthesis is described in the next paragraph.

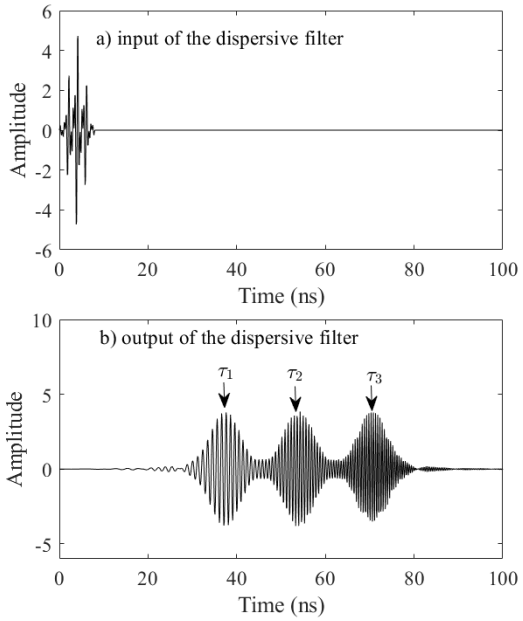

Fig. 6 Input and output of the dispersive filter in the frequency discriminator

Table 1 Optimized parameters for downslope filter

Cell *i*	f_{0i} (MHz)	Q_i
1	800.698	1.1099
2	1368.9	1.2242

Table 2 Optimized parameters for upslope filter

Cell *i*	f_{0i} (MHz)	Q_i
1	1179.95	1.1013
2	1483.33	2.0178

As soon as the filter have the same input and output impedance, the cascade of the filter will result for the group delay as the sum of the group delay of each cell. For both filters, the individual group delay of each cell as well as the expected group delay of the cascade are presented in Figures 7 and 8. From these figures, we can observe that the group delays have the following characteristics:

- For the downslope dispersive filter, it is linear from 780 MHz up to 1.9 GHz with a downslope of -1 ns/GHz.
- For the upslope dispersive filter, it is linear form 500 MHz up to 1.3 GHz with an upslope of 1.25 ns/GHz.

$$H_i(j\omega) = \frac{-\omega^2 - j\omega\frac{\omega_{0i}}{Q_i} + \omega_{0i}^2}{-\omega^2 + j\omega\frac{\omega_{0i}}{Q_i} + \omega_{0i}^2} \tag{11}$$

$$\tau_i(\omega) = 2\omega_{0i}Q_i \frac{\omega^2 + \omega_{0i}^2}{\omega^2\omega_{0i}^2 + Q_i^2(\omega^2 - \omega_{0i}^2)^2} \tag{12}$$

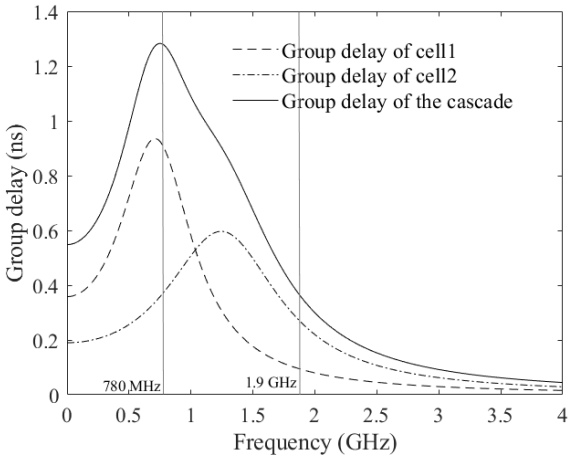

Fig. 7 Group delay of each cell and group delay of the cascade cell1+cell2 for downslope dispersive filter

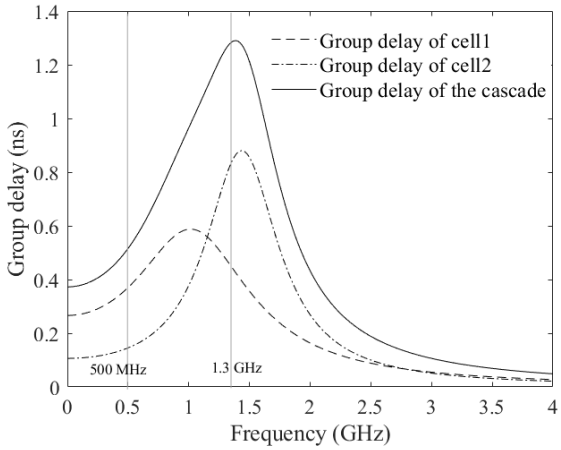

Fig. 8 Group delay of each cell and group delay of the cascade cell1+cell2 for upslope dispersive filter

3.2. Components calculation

The passive topology used for the design of each second-order all-pass cell is presented in Figure 9. We selected the bridge-T topology as it is a classical topology to design second-order filter as for example in [34]. To obtain the wanted group delay based on the values of f_{0i} and Q_i, we use the formulas provided in [35], which are

$$L_1 = \frac{RQ_i}{\omega_{0i}^2} \tag{13}$$

$$L_2 = \frac{R}{Q_i \omega_{0i}^2} \tag{14}$$

$$C_1 = \frac{1}{RQ_i \omega_{0i}} \tag{15}$$

$$C_2 = \frac{Q_i}{\omega_{0i} R} \tag{16}$$

where R is the wanted value of input and output impedance, here 50 Ω. Resulting calculated nominal values are synthesized in Table 3 and 4 together with the selected SMD components which have been selected. These selected components are the one with the closest value available in the market. The view of one cell is presented in Figure 10.

Table 3 Ideal vs SMD components values for downslope filter

	Cell i	$2L_2$ (nH)	$L_1/2$ (nH)	C_1 (pF)	$(C_2-C_1)/2$ (pF)
Ideal	1	17.6	5.5	3.6	0.4
	2	10.5	3.2	2	0.24
SMD	1	18	4.7	3.3	0.5
	2	10	2.7	2.2	0.3

Table 4 Ideal vs SMD components values for upslope filter

	Cell i	$2L_2$ (nH)	$L_1/2$ (nH)	C_1 (pF)	$(C_2-C_1)/2$ (pF)
Ideal	1	13.3	3.42	2.66	0.0352
	2	5.32	5.41	1.06	1.63
SMD	1	13	2.7	3.3	0
	2	6.8	4.7	1	1.8

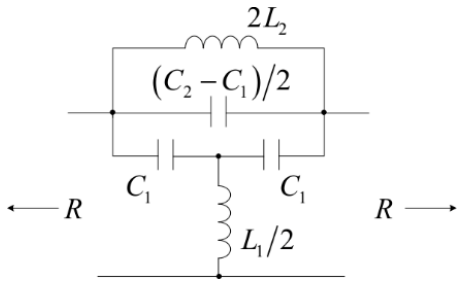

Fig. 9 Selected passive bridge-T topology for the second-order all-pass filter

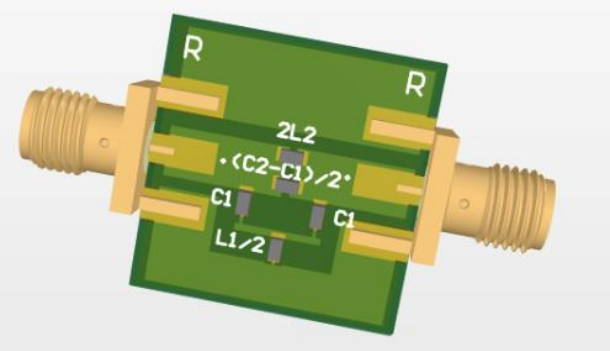

Fig. 10 View of one bridge-T cell with SMA connectors

4. Measurement of the Dispersive Filters and Discussion

4.1. Measurement results

A picture of the downslope prototype is presented in Figure 11. The cells are cascaded with SMA male connectors and the circuit has been measured using a Rhode and Schwarz ZND vector network analyzer. Calibration has been done with N connectors and TOSM (Through-Open-Short-Match) Cal-Kit. For measurement, two N/SMA adapters have been added after calibration and are connected to the VNA through 60 cm Radiall cables. Group delay is measured using aperture width of 5%. For the downslope dispersive filter, the resulting group delay is presented in Figure 12 and for the upslope dispersive filter the group delay is presented in Figure 13. In both cases, the measured group delay totally fits with the ideal expected group delay. It can be noticed that a delay offset exists and is due to the two N/SMA adapters and the length of the lines in the prototype. For the downslope dispersive filter, the bandwidth of linear-shape of the group delay is as predicted from 780 MHz up to 1.9 GHz and goes on to 2.3 GHz. As predicted the downslope of the group delay is -1 ns/GHz. For the upslope dispersive filter, the bandwidth of linear-shape of the group delay is from 500 MHz up to 1.3 GHz. The upslope of the group delay is 1.25 ns/GHz.

Fig. 11 Two-cells prototypes for downslope and upslope dispersive filters

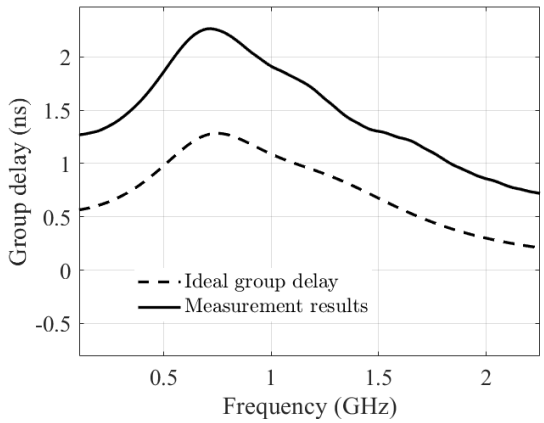

Fig. 12 Measured group delay compared to ideal group delay for the downslope dispersive filter

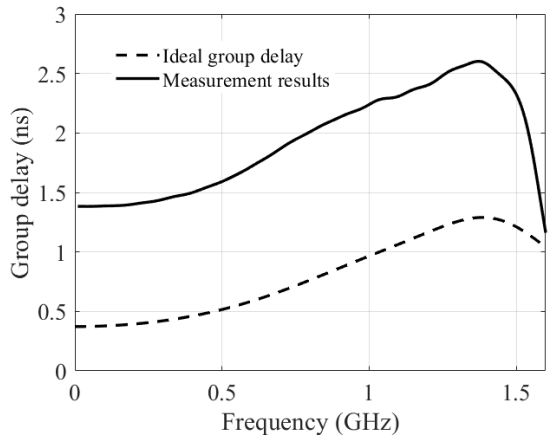

Fig. 13 Measured group delay compared to ideal group delay for the upslope dispersive filter

The S-parameters are presented in Figure 14 and Figure 15. S-parameters show a suitable matching up to 1.8 GHz for the downslope dispersive filter with S_{11} and S_{22} parameters remaining below -10 dB, and for the upslope dispersive filter a suitable matching up to 1 GHz with S_{11} and S_{22} parameters remaining below -10 dB.

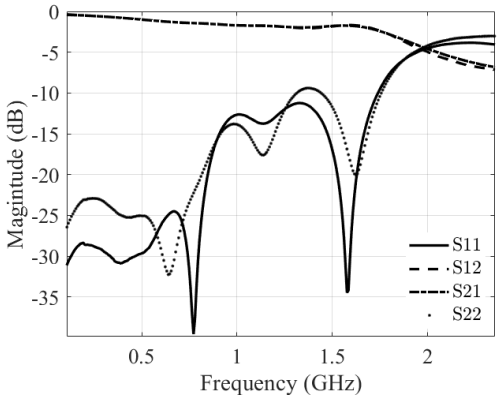

Fig. 14 Measured S-parameters of the cascaded cells for the downslope dispersive filter

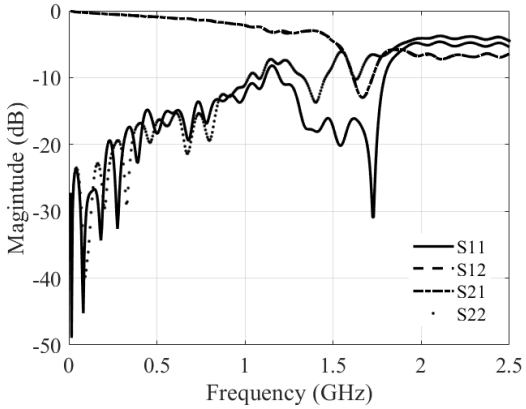

Fig. 15 Measured S-parameters of the cascaded cells for the upslope dispersive filter

4.2. Comparison with the state of the art and discussion

In terms of performance, our work can be compared with the state-of-the-art mainly through two different angles: the performance of the dispersive filter and its technology and the performance of the optimization method to obtain a linear group delay phaser.

Regarding the performance of the dispersive filter we should first recall that there is a lot of possibilities to implement phasers and more generally delay cells: SAW filters, LC filters on PCBs, integrated circuits, microstrip lines, waveguides, optical devices. The comparison here will be restricted to PCBs with lumped components and integrated circuits implementation having a linear group delay characteristic. In the previously published work [36], dispersive filters are implemented with SMD components on PCBs. The authors implemented linear group delay filters with upslope and downslope characteristics. They employed a cascade of two up to nine second order all-pass filters to obtain different values of dispersion and slope in a given bandwidth. Using 9 cascaded stages they obtain an upslope of +/- 6ns/GHz in the bandwidth 500 MHz – 1 GHz. When using only two stages, they obtain, various upslope group delay characteristics between 1.5 ns/GHz with a good linearity up to 8 ns/GHz with a poor linearity

in the same bandwidth. With integrated circuits, the bandwidth of linear group delay is much wider, because L and C elements must be small to be integrated. It also leads to small dispersion. For example, in [28], the bandwidth is 12 – 16 GHz, but the maximum dispersion is only 1.2 ns leading to an upslope of group delay characteristic of 0.375 ns/GHz. In [38], the bandwidth is of 0.4 – 4 GHz and the maximum dispersion is 1.2 ns leading to a slope of 0.3 ns/GHz. To compensate for this bandwidth dispersion trade-off, an interesting technique is to build a loop with the dispersive filter as presented in [21]. With this technique, the group delay slope is increased at each turn in the loop.

Beside the bandwidth/dispersion trade-off highlighted before, there is also a limitation of the approach of cascading cells. The limitation comes from the fact that it assumes that the matching is ideal between the cascaded cells, and this assumption is never totally true in practice resulting in damaged linearity of the group delay.

Concerning the performance of the optimization method itself there is no particular limitations. It has been proved in [17] that it is robust compared to the other methods, thanks to an optimized initialization of the group delay. It has been showed that it is possible to optimize mathematically up to 21 cells, which is much more than what is needed, or achievable when considering practical implementations.

5. CONCLUSION

In this paper two dispersive filters with downslope and upslope linear group delay characteristic have been designed based on a cascade of two optimized second order passive all-pass cells. Measurement results show for one filter a useful bandwidth from 780 MHz up to 1.9 GHz, with a downslope -1 ns/GHz and for the other filter a useful bandwidth from 500 MHz up to 1.3 GHz, with an upslope 1.25 ns/GHz. The targeted applications for these kinds of filters are described: analog pulse compression radar, analog chirp Fourier transformer and frequency discriminator. While there is still space for improving linearity, measurement results indicate that these kinds of dispersive filters can be successfully implemented using lumped elements in lower gigahertz range of frequencies.

REFERENCES

[1] H. Meliani, E. Avignon-Meseldzija, J. Anastasov, D. Milic and P. M. Ferreira, "Design of a Passive Dispersive Filter for Analog Pulse Compression Radar," In Proceedings of the 16th International Conference on Advanced Technologies, Systems and Services in Telecommunications (TELSIKS), Nis, Serbia, 2023, pp. 262-265.

[2] M. M. Safari and J. Pourrostam, "The role of analog signal processing in upcoming telecommunication systems: Concept, challenges, and outlook", *Signal Process.*, vol. 220, no. February, p. 109446, 2024.

[3] Z. Jouni, T. Soupizet, S. Wang, A. Benlarbi-Delai, P. M. Ferreira, "RF neuromorphic spiking sensor for smart IoT devices", *Analog Integr Circ Sig Process*, vol. 117, pp. 3–20, 2023.

[4] X. Chao and Q. Li, "A 128-GS/s Timing-Robust Sampling Architecture Exploiting Analog FFT", In Proceedings of the IEEE International Symposium on Circuits and Systems (ISCAS), Monterey, CA, USA, 2023, pp. 1–4.

[5] C. Caloz, S. Gupta, Q. Zhang, and B. Nikfal, "Analog signal processing: a possible alternative or complement to dominantly digital radio schemes", *IEEE Microw. Mag.*, vol. 14, no. 6, pp. 87–103, Sep. 2013.

[6] C. Campbell, Surface acoustic wave devices and their signal processing applications. Elsevier, 2012.

[7] K. Kashiwagi, Y. Kodama, Y. Tanaka, and T. Kurokawa, "Tunable pulse compression technique using optical pulse synthesizer", In Proceedings of the Conference on Lasers and Electro-Optics and 2009 Conference on Quantum electronics and Laser Science Conference, 2009, pp. 1–2.

[8] C. Song, J. Qian, M. Lei, Z. Zheng, S. Huang, and X. Gao, "A chirprate- tunable microwave photonic pulse compression system for multioctave linearly chirped microwave waveform", *IEEE Photonics J.*, vol. 11, no. 2, pp. 1–13, 2019.

[9] J. A. de França Ferreira, E. Avignon-Meseldzija, P. Maris Ferreira, P. Benabes, "Design of integrated all-pass filters with linear group delay for analog signal processing applications", *Int. J. Circuit Theory Applic*., Wiley, vol. 48, no. 5, pp. 658–673, 2020.

[10] P. Keerthan and K. J. Vinoy, "Design of cascaded all pass network with monotonous group delay response for broadband radio frequency applications", *IET Microw. Antennas Propag.*, vol. 10, no. 7, pp. 808–815, May 2016.

[11] E. Avignon-Meseldzija, Jelena Anastasov, Dejan N Milic, "A linear group delay filter with tunable positive slope for analog signal processing", *Int. J. Circuit Theory Applic*, Wiley, vol. 49, no. 5, pp. 1307–1326, 2021.

[12] R. Gómez-García, L. Yang, M. Malki and J. -M. Muñoz-Ferreras, "Flat-Group-Delay RF Planar Filters With Transmission Zeros Using Transversal Circuits", *IEEE Trans. Circuits Syst. I: Regul. Pap.*, vol. 70, no. 10, pp. 3843–3856, Oct. 2023.

[13] G. Yang, D. Lee and B. -W. Min, "Cascaded Reflection-Type Group Delay Controller With a Wideband Flat Group Delay", *IEEE Microw.Wirel. Tech.. Lett.*, vol. 33, no. 7, pp. 979–982, July 2023.

[14] S. Gupta, A. Parsa, E. Perret, R. V. Snyder, R. J. Wenzel, and C. Caloz, "Group-delay engineered noncommensurate transmission line all-pass network for analog signal processing", *IEEE Trans. Microw. Theory Techn.*, vol. 58, no. 9, pp. 2392–2407, Sep. 2010.

[15] T. Henk, "The generation of arbitrary-phase polynomials by recurrence formulae", *Int. J. Circuit Theory Applic* , vol. 9, no. 4, pp. 461–478, Oct. 1981.

[16] P. J. Osuch and T. Stander, "A geometric approach to group delay network synthesis", *Radioengineering*, vol. 25, no. 2, pp. 351–864, Jun.2016.

[17] D. N. Milic, E. Avignon-Meseldzija, J. A. Anastasov, H. Meliani, and A. Benlarbi-Delaï, "A robust algorithm for the design of wideband positive-slope linear group delay filters", *IEEE Trans. Circuits Syst. I: Regul. Pap* , vol. 69, no. 10, pp. 4258–4271, 2022.

[18] X. Wang, A. Akbarzadeh, L. Zou, and C. Caloz, "Real-Time Spectrum Sniffer for Cognitive Radio Based on Rotman Lens Spectrum Decomposer", *IEEE Access*, vol. 6, pp. 52366–52373, Sep. 2018.

[19] P. Sepidband and K. Entesari, "A CMOS Real-Time Spectrum Sensor Based on Phasers for Cognitive Radios", *IEEE Trans. Microw. Theo. Tech.*, vol. 66, no. 3, pp. 1440–1451, 2018.

[20] Q. Zhang, B. Nikfal, and C. Caloz, "High-Resolution Real-Time Spectrum Sniffer for Wireless Communication", In Proceedings of the IEEE International Symposium on Electromagnetic Theory, 20–24 May 2013.

[21] B. Nikfal, S. Gupta and C. Caloz, "Increased Group-Delay Slope Loop System for Enhanced-Resolution Analog Signal Processing", *IEEE Trans. Microw. Theo. Tech.*, vol. 59, no. 6, pp. 1622–1628, June 2011.

[22] M. A. Jack, P. M. Grant and J. H. Collins, "The theory, design, and applications of surface acoustic wave Fourier-transform processors", In Proceedings of the IEEE, April 1980, vol. 68, no. 4, pp. 450–468.

[23] O. W. Otto, "The Chirp Transform Signal Processor", 1976 Ultrasonics Symposium, Annapolis, MD, USA, 1976, pp. 365–370.

[24] D. Gangopadhyay, A. Y. Chen and D. J. Allstot, "Analog Chirp Fourier Transform for high-resolution real-time wideband RF spectrum Analysis", In Proceedings of the 2011 IEEE International Symposium of Circuits and Systems (ISCAS), Rio de Janeiro, Brazil, 2011, pp. 2441–2444.

[25] Joao Alberto de França Ferreira, PhD manuscript "Contribution to the Design of a Real-Time Foruier Transformer in Integrated Technology", 2019. https://theses.hal.science/tel-02494464

[26] L. Zou, S. Gupta, and C. Caloz, "Real-time dispersion code multiple access for high-speed wireless communications", *IEEE Trans. Wirel. Commun.*, vol. 17, no. 1, pp. 266–281, 2018, doi: 10.1109/TWC.2017.2765304

[27] I. Mondal and N. Krishnapura, "Expansion and compression of analog pulses by bandwidth scaling of continuous-time filters", *IEEE Trans. Circuits Syst. I: Regul. Pap.*, vol. 65, no. 9, pp. 2703–2714, Sep. 2018.

[28] B. Xiang, A. Kopa, Z. Fu and A. B. Apsel, "An integrated Ku-band nanosecond time-stretching system using improved dispersive delay line (DDL)", In Proceedings of the IEEE 12th Topical Meeting on Silicon Monolithic Integrated Circuits in RF Systems, Santa Clara, CA, USA, 2012, pp. 151–154.

[29] X. Zhao, S. Xiao and Y. Sun, "A Fully Electronic Time Reversal Mirror System Based on Temporal Imaging," *IEEE Access*, vol. 7, pp. 16711–16717, 2019.

[30] Y. Kim, T. J. Reck, M. Alonso-delPino, T. H. Painter, H.-P. Marshall, E. H. Bair, J. Dozier, G. Chattopadhyay, K.-N. Liou, M.-C. F. Chang, and A. Tang, "A ku-band cmos fmcw radar transceiver for snowpack remote sensing", *IEEE Trans. Microw. Theo. Tech.*, vol. 66, no. 5, pp. 2480–2494, 2018.

[31] I. M. Milosavljevic, D. P. Glavonjic, D. P. Krcum, S. P. Jovanovic, V. R. Mihajlovic, and V. M. Milovanoví´c, "A 55–64-GHz fully integrated miniaturized FMCW radar sensor module for short-range applications", *IEEE Microw.Wirel. Compon. Lett.*, vol. 29, no. 10, pp. 677–679, 2019.

[32] P. Tortoli, F. Guidi, and C. Atzeni, "Digital vs. SAW matched filter implementation for radar pulse compression", In Proceedings of the IEEE Ultrasonics Symposium, 1994, vol. 1, pp. 199–202.

[33] A. Williams and F. J. Taylor, Electronic Filter Design Handbook, Fourth Edition (McGraw-Hill Handbooks). McGraw-Hill Professional, 2006. (Chapter 7, formula 7-6). ISBN: 9780071471718

[34] Suhash C. Dutta, "A new lumped element bridged-T absorptive band-stop filter", *Facta Universitatis (NIS) – Series : Electronics and Energetics, vol*. 30, pp. 179–185, June 2017.

[35] G. Lissorgues and C. Berland, "Synthèse des filtres LC", Techniques de l'ingénieur, no. E130, Sep. 2015, doi: 10.51257/a-v1-e130

[36] P. Keerthan and K. J. Vinoy, "Design of cascaded all pass network with monotonous group delay response for broadband radio frequency applications", *IET Microw., Antennas P.*, vol. 10, no. 7, pp. 808–815, 2016.

[37] P. Keerthan, R. Kumar and K. J. Vinoy, "Wide-band real-time frequency measurement using compressive receiver," In Proceedings of the International Conference on Signal Processing and Communications (SPCOM), Bangalore, India, 2016, pp. 1–5.

[38] B. Xiang, X. Wang and A. B. Apsel, "A Reconfigurable Integrated Dispersive Delay Line (RI-DDL) in 0.13µm CMOS Process", *IEEE Trans. Microw. Theo. Tech.*, vol. 61, no. 7, pp. 2610–2619, July 2013.